A calculation of the phonon-drag thermopower of a 1D electron gas

A calculation of the phonon-drag thermopower of a 1D electron gas

S S Kubakaddi† and P N Butcher

Department of Physics, University of Warwick, Coventry CV4 7AL, UK

Abstract. The theory of phonon-drag thermopower S_g is given for a quasi-1D electron gas in a GaAs heterostructure. The coupling of the electrons to 3D phonons is considered through acoustic deformation potential and piezoelectric fields. An expression for S_g is given which may be used for quasi-1D wires of different geometries. Numerical results are presented for both the screened and the unscreened value of S_g for cylindrical wires in the temperature range 1–10 K. For temperatures $T \geq 2$ K the major contribution to S_g comes from the deformation potential scattering but for $T < 2$ K the contribution to S_g due to piezoelectric scattering is significant. Screening reduces S_g by 40%. S_g increases as the density of electrons decreases and curves of S_g/T^3 against T show maxima. The overall behaviour is dominated by the 3D character of the phonon system and is similar to that found previously for a quasi-2D electron gas coupled to 3D phonons.

1. Introduction

In recent years there has been growing interest in the experimental (Fletcher *et al* 1986, 1988, Gallagher *et al* 1987, Ruf *et al* 1988) and theoretical (Cantrell and Butcher 1987a, b, Smith and Butcher 1989, Lyo 1988) study of the thermopower S_g of a quasi-2D (Q2D) electron gas in GaAs heterostructures and silicon inversion layers. Traditionally, the study of S has been used to probe electronic structure and scattering mechanisms in solids because it is sensitive to the energy dependence of the scattering mechanisms. At liquid-helium temperatures it is well known that there are two contributions to S. One is due to the diffusion of carriers through the specimen when a temperature gradient ∇T is present. This is the 'diffusion' thermopower S_d. The other arises because ∇T produces a phonon momentum current which drags electrons with it as a result of electron–phonon interactions. This is the 'phonon-drag' thermopower S_g. The total thermopower S may be written as

$$S = S_d + S_g. \tag{1}$$

The experimental measurements of S and its theoretical explanation in a Q2D electron gas confirm the dominance of the contribution of S_g to S at liquid-helium temperature until T falls below 1 K (Ruf *et al* 1988).

There is also growing interest in the study of the electronic structure and transport properties of quasi-1D (Q1D) systems in which the electron gas is free to move in only one

† Permanent address: Department of Physics, Karnatak University, Dharwad 580003, India.

direction and is confined in the other two. QID electron gases have been produced in silicon MOSFETs (Skocpol *et al* 1982, Wheeler *et al* 1982, Kwasnick *et al* 1984, Warren *et al* 1986) and in GaAs heterostructures (Berggren *et al* 1986, van Houten *et al* 1987, Cibert *et al* 1986, van Wees *et al* 1988). The diffusion thermopower of a QID electron gas has been studied by Kearney and Butcher (1986) and Kubakaddi and Mulimani (1985). In this paper, we give the Boltzmann transport theory of S_g for QID electrons in a GaAs wire coupled to 3D phonons in the surrounding medium by making appropriate modifications of the analysis of Cantrell and Butcher (1987a, b). Electrons are assumed to interact with acoustic phonons through both deformation potential and piezoelectric fields. A very recent calculation of S_g for a Q2D electron gas in GaAs heterostructures (Lyo 1988) shows that the contribution to S_g from the piezoelectric scattering dominates for temperatures below 3 K.

In § 2, we give the Boltzmann transport theory of S_g in a form which is applicable to wires of different geometries. In § 3, we give explicit expressions for S_g for cylindrical wires. In § 4, we present numerical results both with and without screening included.

2. Boltzmann transport theory of S_g

We model our QID quantum wire as an electron system with periodic boundary conditions in the z direction and confined by potentials in the x and y directions. The confining potentials decide the geometry of the wire. We give the theory without specifying the form of the confining potential. Let us write the one-electron wavefunction $\psi_{kmn}(x, y, z)$ in the QID systems as

$$\psi_{kmn}(x, y, z) = (l)^{-1/2} \exp(ikz)\Phi_{mn}(x, y) \tag{2}$$

where positive integers m and n specify the (mn)th 1D sub-band. In (2), k is the wavenumber in the z direction, l is the length of the wire and $\Phi_{mn}(x, y)$ is the normalised sub-band wavefunction. The corresponding eigenvalue is

$$\varepsilon_{mn}(k) = \varepsilon_{mn} + \varepsilon_k \tag{3}$$

where the ε_{mn} are the energies of the sub-band minima and ε_k is the free-electron energy in the z direction with effective mass m^*.

To calculate S, we recall that it is defined by the relation

$$E = S \, dT/dz \tag{4}$$

under open-circuit conditions. Here dT/dz is the temperature gradient in the direction of the wire and E is the corresponding EMF. When the (total) current J in the wire does not vanish, we may write (Barnard 1972)

$$J = -(L_{EE})_{zz}E + (L_{ET})_{zz} \, dT/dz \tag{5}$$

where $(L_{EE})_{zz}$ is the conductivity σ and, from (4), $(L_{ET})_{zz} = -\sigma S$. Hence, when the EMF is reduced to zero by allowing current to flow, the current due to the temperature gradient is

$$J = -\sigma S \, dT/dz. \tag{6}$$

The current associated with the wavefunctions (2) is obtained by evaluating

$$J = \frac{-2|e|}{l} \sum_{m,n,k} f_{mn}(k)v_{mn}(k). \tag{7}$$

Here $|e|$ is the magnitude of the electronic charge, $f_{mn}(k)$ the electron distribution

function and $v_{mn}(k)$ the group velocity of the electrons in the (mn)th sub-band. The factor of 2 accounts for spin. We obtain S by comparing (6) and (7) and S_g is that part of the S coming from the departure of the phonon distribution function from its thermal equilibrium value.

To evaluate the current, $f_{mn}(k)$ is obtained from the coupled electron and phonon Boltzmann equations, by linearising them, in the relaxation time approximation. Phonon–phonon interactions are assumed to dominate the scattering of phonons and are described by a phonon relaxation time $\tau_p(Q)$. It is also assumed that, at very low temperatures of our interest, the electron scattering is dominated by static defects and may be described by the electron relaxation time $\tau_{mn}(\varepsilon_k)$. The scattering due to the electron–phonon interaction is assumed to be weak as far as relaxation processes are concerned. However, it is the interaction which produces S_g and is our main concern here. At very low temperatures, we can neglect all but the acoustic phonons of energy $\hbar\omega_{Qs}$ and wavevector $Q = (q_x, q_y, q_z)$ in the sth mode. The electron–phonon interaction is due to the acoustic deformation potential and piezoelectric fields. The electron transition rate, due to either of these two scattering processes, at which the electron will transfer from state (m, n, k) to (i, j, k') by absorbing a phonon is given by

$$P_{Qs}^a(m, n, k; i, j, k') = (2\pi/\hbar)N_{Qs}|M(m, n, k; i, j, k')|^2$$

$$\times \delta[\varepsilon_{ij}(k') - \varepsilon_{mn}(k) - \hbar\omega_{Qs}]\delta_{k', k+q_z}. \tag{8}$$

Here $M(m, n, k; i, j, k')$ is the matrix element of the screened electron–phonon interaction. It is well known that only longitudinal modes (s = l) are involved in the deformation potential scattering whereas both longitudinal and transverse (s = t) modes are involved in the piezoelectric scattering. The matrix element

$$|M(m, n, k; i, j, k')|_{\mathrm{def}}^2 = [\hbar\omega_{Ql}E_1^2/2\rho Vv_l^2\varepsilon^2(q_z)]|F_{mn}^{ij}(q_x, q_y)|^2 \tag{9}$$

arises from deformation potential scattering and

$$|M(m, n, k; i, j, k')|_{\mathrm{piezo}}^2 = [(eh_{14})^2/2\rho V\varepsilon^2(q_z)]$$

$$\times |(\hbar\omega_{Ql}/v_l^2)(A_1/Q^2) + (2\hbar\omega_{Qt}/v_t^2)(A_t/Q^2)||F_{mn}^{ij}(q_x, q_y)|^2 \tag{10}$$

is due to piezoelectric scattering. The quantities ρ, V, E_1 and h_{14} are, respectively, the mass density, volume, acoustic deformation potential constant and piezoelectric constant. $\varepsilon(q_z)$ is the dielectric function of the Q1D electron gas and the form factor $|F_{mn}^{ij}(q_x, q_y)|^2$ is given by

$$|F_{mn}^{ij}(q_x, q_y)|^2 = \left|\int\int \Phi_{ij}^*(x, y)\Phi_{mn}(x, y) \exp[i(q_xx + q_yy)] \, \mathrm{d}x \, \mathrm{d}y\right|^2. \tag{11}$$

Finally, the quantities A_1 and A_t are, respectively (Price 1982),

$$A_1 = 9q_\perp^4 q_z^2/2Q^6 \tag{12}$$

and

$$A_t = (8q_\perp^2 q_z^4 + q_\perp^6)/4Q^6 \tag{13}$$

with

$$q_\perp^2 = q_x^2 + q_y^2. \tag{14}$$

The linearised electron and phonon Boltzmann equations are solved for $f_{mn}(k)$ with

(8) substituted for $P_{Qs}^a(m, n, k; i, j, k')$ and $E = 0$. We then calculated J from (7) and pick out the part arising from the perturbation of the phonon distribution by dT/dz. Then, by comparing (6) and (7), the S_g for the quantum wire when several sub-bands are occupied is found to be

$$S_g = \frac{2|e|}{l\sigma k_B T^2} \sum_{\substack{i,j,k' \\ m,n,k}} \sum_{Q,s} \hbar \omega_{Qs} f_{mn}^0(\varepsilon_k)[1 - f_{ij}^0(\varepsilon_{k'})] P_{Qs}^{a0}(m, n, k; i, j, k') \tau_p(Q, s)$$

$$\times v_{sz}[\tau_{mn}(\varepsilon_k) v_{mn}(k) - \tau_{ij}(\varepsilon_{k'}) v_{ij}(k')] \tag{15}$$

where v_{sz} is the z component of the velocity of sound, $P_{Qs}^{a0}(m, n, k; i, j, k')$ is P_{Qs}^a with N_{Qs} replaced by its thermal equilibrium value N_{Qs}^0 (given by the Bose distribution at temperature T) and $f_{mn}(\varepsilon_k)$ is the Fermi–Dirac distribution function at T, for a sub-band of energy $\varepsilon_{mn}(k)$, with chemical potential ε_F.

In order to study the dependence of S_g on T, ε_F and the transverse dimensions of the wire, we evaluate (15) when only the ground sub-band is occupied. The phonon relaxation time is assumed to be limited by boundary scattering. Then $\tau_p(Q, s) = L/v_s$, where L is the appropriate sample dimension and v_s is an average velocity of sound which are taken to be independent of Q. Since we are concerned only with the ground sub-band, we drop all the sub-band subscripts from (15). When this is done, we are left with a summation over k', k and Q. The summation over k' is carried out making use of the Kronecker δ-function in (8), i.e. k' is replaced by $k + q_z$. The integration over k is carried out by noting that, for small $\hbar \omega_{Qs}$,

$$f^0(\varepsilon_k)[1 - f^0(\varepsilon_k + \hbar \omega_{Qs})] = \{\hbar \omega_{Qs}/[1 - \exp(-\beta \hbar \omega_{Qs})]\}\delta(\varepsilon_k - \varepsilon_F) \tag{16}$$

where $\beta = (k_B T)^{-1}$. This gives

$$S_g = \frac{|e|m^*L}{\sigma k_B T^2 \pi \hbar^2 k_F} \sum_{Q,s} \frac{(\hbar \omega_{Qs})^2}{v_s[1 - \exp(-\beta \hbar \omega_{Qs})]} \{P_{Qs}^{a0}(k_F, k_F + q_z)$$

$$\times v_{sz}[\tau(\varepsilon_F) v(k_F) - \tau(\varepsilon_F + \hbar \omega_{Qs}) v(k_F + q_z)] + P_{Qs}^{a0}(-k_F, -k_F + q_z)$$

$$\times v_{sz}[\tau(\varepsilon_F) v(-k_F) - \tau(\varepsilon_F + \hbar \omega_{Qs}) v(-k_F + q_z)]\} \tag{17}$$

where $k_F = n_0 \pi/2$ is the Fermi wavevector with n_0 denoting the density of electrons per unit length and

$$v_{sz} = v_s q_z/|Q|. \tag{18}$$

Moreover, the electron relaxation time due to short-range static defects has been calculated by Kearney and Butcher (1986) who find that $\tau(\varepsilon_k) = C\varepsilon_k^{1/2}$, where C is independent of energy. We sum over Q by writing the summation over q_x, q_y and q_z. The summation over q_z is replaced by the integral

$$\sum_{q_z} \rightarrow \frac{l}{2\pi} \int_{-\infty}^{\infty} dq_z \tag{19}$$

and we use the Dirac δ-function in (8), dropping $\hbar \omega_{Qs}$ compared with ε_F in its argument,

to integrate over q_z. The neglect of $\hbar\omega_{Qs}$ compared with ε_F is justified in §4. The integration over q_z then gives

$$S_g = -\frac{m^* L l}{n_0 |e| \pi k_B T^2 \hbar^3} \sum_{q_x, q_y, s} \frac{v_s \gamma_s G(\gamma_s)}{\sinh^2(\beta\gamma_s/2)} |M(k_F, -k_F)|^2 \tag{20}$$

where

$$\gamma_s = 2\hbar v_s k_F [1 + (q_\perp/2k_F)^2]^{1/2} \tag{21}$$

and

$$G(\gamma_s) = (1 + \gamma_s/\varepsilon_F)^{1/2} + 1. \tag{22}$$

We have in (20) the general expression for S_g which can be used to evaluate S_g for quantum wires of different geometries by appropriate choice of the ground sub-band wavefunction in (11).

3. S_g for a cylindrical wire

To illustrate the behaviour of S_g, we consider a wire of circular cross section with radius R. For this system the ground sub-band wavefunction is (with $m = 1$, $n = 0$ in (2))

$$\Phi(r) = \begin{cases} J_0(k_{10}r)/(\pi R^2)^{1/2} J_1(k_{10}R) & \\ 0 & \end{cases} \quad \text{for} \begin{cases} r \leqslant R \\ r > R \end{cases} \tag{23}$$

and the energy eigenvalue is

$$\varepsilon_{10} = \hbar^2 k_{10}^2/2m^* \tag{24}$$

where $r = (x^2 + y^2)^{1/2}$ and $k_{10}R$ is the first zero of the Bessel function $J_0(x)$. Using (23) in (11), we obtain the following expression:

$$S_{gd} = \frac{4E_1^2 L m^{*2} k_F v_l}{n_0 \pi^2 |e| k_B T^2 \rho \hbar \varepsilon^2(2k_F)} \int_0^\infty \frac{x(1 + x^2) G(\gamma_l) |F(2k_F x, R)|^2 \, dx}{\sinh^2(\beta\gamma_l/2)} \tag{25}$$

for acoustic deformation potential scattering and

$$S_{gp} = \frac{|e| h_{14}^2 L m^{*2} k_F^2}{2n_0 \pi^2 k_B T^2 \rho \hbar \varepsilon^2(2k_F)}$$

$$\times \int_0^\infty dx \left(\frac{9v_l G(\gamma_l) x^4}{\sinh^2(\beta\gamma_l/2)} + \frac{v_t G(\gamma_t)(8x^2 + x^6)}{\sinh^2(\beta\gamma_t/2)} \right) \frac{x|F(2k_F x, R)|^2}{(1 + x^2)^3}. \tag{26}$$

In deriving (25) and (26) we have replaced the summations over q_x and q_y by an integral in polar coordinates with $x = q_\perp/2k_F$.

4. Numerical results and discussion

In this section, we present numerical results for a Q1D cylindrical GaAs quantum wire obtained using the following material parameters: $m^* = 0.067m_0$, $\rho = 5.3 \text{ g cm}^{-3}$, $v_l = 5.1 \times 10^5 \text{ cm s}^{-1}$, $v_t = 3.04 \times 10^5 \text{ cm s}^{-1}$, $E_1 = 8.0 \text{ eV}$, $h_{14} = 1.2 \times 10^7 \text{ V cm}^{-1}$ and $K_s =$
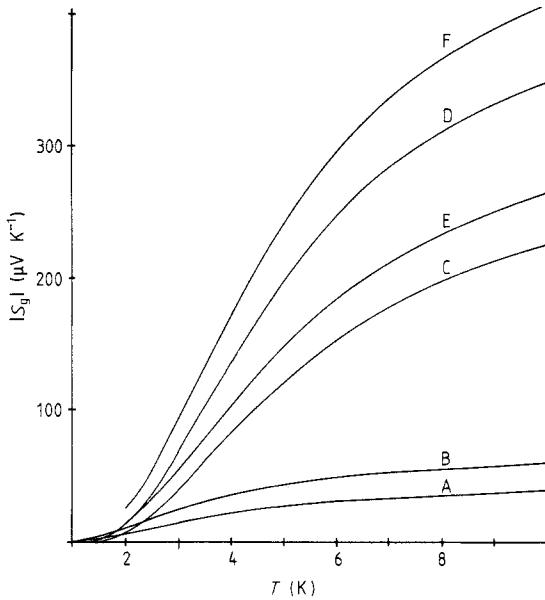
Figure 1. Plots of S_g against T for a cylindrical quantum wire of radius 100 Å and electron density $10^6 \mathrm{cm}^{-1}$: curve A, screened piezoelectric scattering; curve B, unscreened piezoelectric scattering; curve C, screened deformation potential scattering; curve D, unscreened deformation potential scattering; curve E, screened total S_g; curve F, unscreened total S_g.

12.9. The sub-band energy minima are determined by the radius of the wire. The ground and first sub-band energy minima are of concern to us. For a wire of radius 100 Å the energy separation of the ground and first sub-band is about 51 meV. The separation decreases with increasing R. Our expressions for S_g are for ε_F lying between the ground and first sub-band minima. For $n_0 \simeq 10^6 \mathrm{cm}^{-1}$, ε_F is 14 meV. We calculate S_g from (25) and (26) for different n_0 and R such that ε_F is always between the two lowest sub-band minima. It is to be noted that the approximation $\hbar\omega_Q \ll \varepsilon_F$ is valid for $n_0 \simeq 10^6 \mathrm{cm}^{-1}$ because $\hbar\omega_Q \simeq 0.5$ meV for $Q \simeq k_F$. When screening is ignored, we set $\varepsilon(2k_F) = 1$. To include screening, we use the temperature-dependent $\varepsilon(2k_F)$ given by Fishman (1986):

$$\varepsilon(2k_F) = 1 + (e^2 m^*/\pi K_s \hbar^2 k_F^3 R^2)[1 - 2K_1(2k_F R)I_1(2k_F R)]\ln(4.535\varepsilon_F/k_B T) \qquad (27)$$

where K_s is the static dielectric constant of the medium. In (27), I_n and K_n are modified Bessel functions of the first and second kind, respectively. To be definite, we set $L = 0.3$ mm in carrying out detailed calculations.

In figure 1, we plot S_g for $n_0 = 1.0 \times 10^6 \mathrm{cm}^{-1}$ and $R = 100$ Å. We give screened and unscreened results for piezoelectric scattering (curves A and B), deformation potential scattering (curves C and D) and the sum of the two (curves E and F). Piezoelectric scattering makes a significant contribution over the entire temperature range and becomes larger than the contribution for deformation potential scattering for $T < 2$ K. For a Q2D electron gas, Lyo (1988) finds that the piezoelectric scattering contribution is the larger of the two below 3 K. However, it should be remembered that, when $T \leqslant 1$ K, we must expect S_d to exceed S_g (Kubakaddi and Mulimani 1985, Kearney and Butcher 1986, Ruf et al 1988).

The effect of screening on S_g is easy to include in the present calculations because it depends only on $\varepsilon(2k_F)$ as given in (27) which is logarithmically dependent on T. For $n_0 = 1.0 \times 10^6 \mathrm{cm}^{-1}$, we find a 43% reduction in S_g at 2 K and a 35% reduction at 10 K. We also note from (27) that $\varepsilon(2k_F)$ increases as k_F decreases.
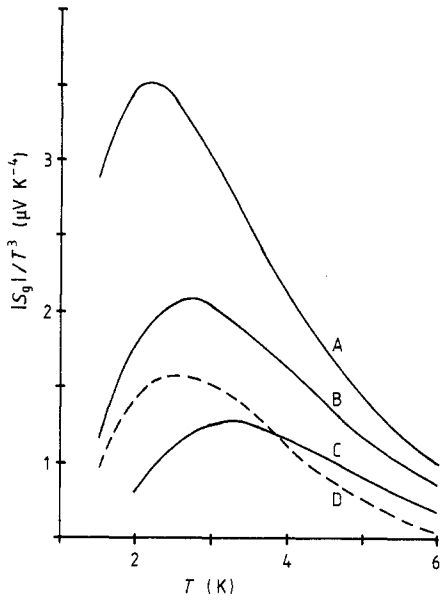
Figure 2. Plots of S_g/T^3 against T: curve A, $R = 100$ Å, $n_0 = 0.8 \times 10^6\,\mathrm{cm}^{-1}$; curve B, $R = 100$ Å, $n_0 = 1.0 \times 10^6\,\mathrm{cm}^{-1}$; curve C, $R = 100$ Å, $n_0 = 1.2 \times 10^6\,\mathrm{cm}^{-1}$; curve D, $R = 150$ Å, $n_0 = 1.0 \times 10^6\,\mathrm{cm}^{-1}$.
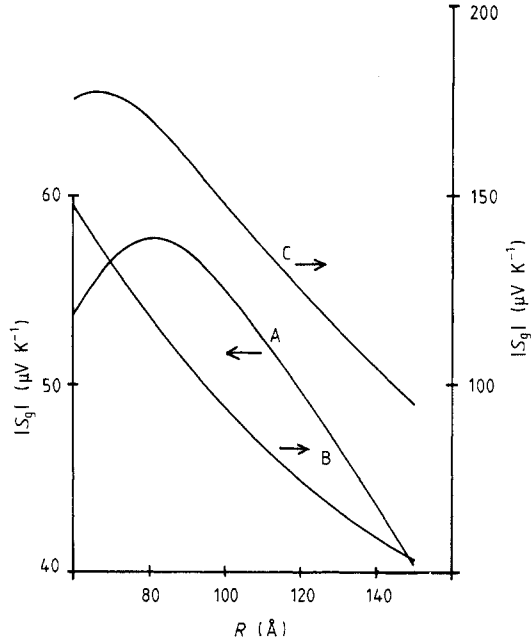
Figure 3. Plots of S_g against R for $n_0 = 1.0 \times 10^6\,\mathrm{cm}^{-1}$: curve A, screened total S_g at 3 K; curve B, unscreened total S_g at 3 K; curve C, screened total S_g at 5 K.

The dependence of S_g on T shown in figure 1 has a T^3 character at intermediate temperatures but a faster (slower) dependence on T at the lower (higher) temperatures in the range considered. Consequently the plots of S_g/T^3 against T exhibit maxima as shown in figure 2 for $R = 100$ Å and $n_0 = 0.8 \times 10^6\,\mathrm{cm}^{-1}$ (curve A), $1.0 \times 10^6\,\mathrm{cm}^{-1}$ (curve B) and $1.2 \times 10^6\,\mathrm{cm}^{-1}$ (curve C). We see that the maximum shifts to lower temperatures and becomes narrower as n_0 decreases. A Q2D electron gas exhibits similar behaviour. It arises from the movement of the dominant phonon wavevector in the integrands of (25) and (26) (Cantrell and Butcher 1986b). Curve D in figure 2 is shown for $n_0 = 1.0 \times 10^6\,\mathrm{cm}^{-1}$ and $R = 150$ Å. Comparing this with curve B for the same value of n_0 and $R = 100$ Å, we see a reduction in the magnitude of the peak but very little change in its location or width.

The R dependence of S_g is exhibited in figure 3 for $n_0 = 1.0 \times 10^6\,\mathrm{cm}^{-1}$ and $T = 3$ K for both screened (curve A) and unscreened (curve B) cases. Curve C shows the results of a screened calculation at 5 K. The screened results exhibit maxima which moves to lower R and broadens as T increases. This behaviour is entirely due to the screening. The unscreened curve B does not have a maximum.

We note that the precise form of the function $G(\gamma_s)$ in (22) is due to the particular energy dependence assumed for the electron relaxation time $(\tau(\varepsilon_k) = C\varepsilon_k^{1/2})$. In the more general case when $\tau(\varepsilon_k) = C\varepsilon_k^p$, we find that

$$G(\gamma_s) = (1 + \gamma_s/\varepsilon_F)^p + 1. \tag{28}$$

When $p = 0$, i.e. when $\tau(\varepsilon_k)$ is constant, $G(\gamma_s) = 2$. Some researchers (Fishman

1986, Lee and Spector 1985) approximate the ground sub-band wavefunction $\Phi(x, y)$ by $(\pi R^2)^{-1/2}$ inside the wire and zero outside it. We have made calculations using this simple approximation and find that it is seriously in error. The value of S_g calculated in this way is 50% below that calculated using the exact wavefunction for the ground sub-band.

We see from this discussion that the overall behaviour of S_g for a Q1D electron gas is very similar to that calculated previously for a Q2D electron gas (Cantrell and Butcher 1986b, Lyo 1988). It is dominated in both cases by the 3D character assumed for the phonons. The calculations will need to be modified considerably if this assumption breaks down. In the Q2D electron gas it yields results in excellent agreement with experimental data for both GaAs heterojunctions (Lyo 1988) and silicon MOSFETs (Smith and Butcher 1988). It should be possible to measure S_g for arrays of weakly coupled quantum wires so that the theory developed here can also be tested against experimental data.

References

Barnard R D 1972 *Thermoelectricity in Metals and Alloys* (London: Taylor and Francis)
Berggren K-F, Thornton T J, Newson D J and Pepper M 1986 *Phys. Rev. Lett.* **57** 1769
Cantrell D G and Butcher P N 1987a *J. Phys. C: Solid State Phys.* **20** 1985
—— 1987b *J. Phys. C: Solid State Phys.* **20** 1993
Cibert J, Petroff P M, Dolan G J, Pearton S J, Gossard A C and English J H 1986 *Appl. Phys. Lett.* **49** 1275
Fishman G 1986 *Phys. Rev.* B **34** 2394
Fletcher R, D'Iorio M, Sachrajda A S, Stoner R, Foxon C and Harris J J 1988 *Phys. Rev.* B **37** 3137
Fletcher R, Maan J C, Ploog K and Weimann G 1986 *Phys. Rev.* B **33** 7122
Gallagher B L, Gibbings C J, Pepper M and Cantrell D G 1987 *Semicond. Sci. Technol.* **2** 456
Kearney M J and Butcher P N 1986 *J. Phys. C: Solid State Phys.* **19** 5429
Kubakaddi S S and Mulimani B G 1985 *J. Appl. Phys.* **58** 3643
Kwasnick R F, Kastner M A, Melngailis J and Lee P A 1984 *Phys. Rev. Lett.* **52** 224
Lee J and Spector H N 1985 *J. Appl. Phys.* **57** 366
Lyo S K 1988 *Phys. Rev.* B **38** 6345
Price P J 1982 *Ann. Phys., NY* **133** 217
Ruf C, Obloh H, Junge B, Gmelin E, Ploog K and Weimann G 1988 *Phys. Rev.* B **37** 6377
Skocpol W J, Jackel L D, Hu E L, Howard R E and Fetter L A 1982 *Phys. Rev. Lett.* **49** 951
Smith M J and Butcher P N 1988 *J. Phys.: Condens. Matter* **1** 1261
Van Houten H, Van Wees B J, Mooij J E, Ross G and Berggren K-F 1987 *Superlatt. Microstruct.* **3** 497
Van Wees B J, Van Houten H, Beenakker C W J, Williamson J G, Kouwenhoven L P, Van der Marel D and Foxon C J 1988 *Phys. Rev. Lett.* **60** 848
Warren A C, Antoniadis D A and Smith H I 1986 *Phys. Rev. Lett.* **56** 1858
Wheeler R G, Choi K K, Goel A, Wisnief R and Prober D E 1982 *Phys. Rev. Lett.* **49** 1674